IEEE Access
Multidisciplinary | Rapid Review | Open Access Journal

Received August 28, 2020, accepted September 12, 2020, date of publication September 18, 2020, date of current version October 6, 2020.

Digital Object Identifier 10.1109/ACCESS.2020.3024774

The Evolution of Trapping Parameters on Three-Layer Oil-Paper of Partial Discharge Degradation for On-Board Traction Transformers

QUANFU LI[1,2], XIAONAN LI[1], YAN YANG[1], (Member, IEEE), YIXUAN LI[1], AND GUANGNING WU[1], (Fellow, IEEE)

[1]School of Electrical Engineering, Southwest Jiaotong University, Chengdu 610031, China
[2]China Shenhua Railway Equipment Company Ltd., Beijing 100120, China

Corresponding author: Xiaonan Li (lixiaonan1989@163.com)

This work was supported in part by the China Shenhua Energy Company Ltd., under Grant SHGF-17-54.

ABSTRACT Trap plays an important role in the charge transportation of three-layer oil-paper and the investigation of trap parameters at different degradation degree is of great significance for further research of the partial discharge (PD) mechanism. This article considers the turn-to-turn structure of on-board traction transformer. A defect model of three-layer oil-paper insulation was designed for PD test. The PD degradation samples are selected from the inception of PD to the breakdown of PD to study the characteristics of surface potential decay on degradation samples by using isothermal surface potential decay method. Given that, the trap distribution at different degradation stages was calculated and its influence on PD characteristics was investigated. The result shows that AC fluctuation voltages caused by inter-harmonic has a great influence on PD distribution, surface charge distribution and trap distribution. With the increase of degradation, the decay rate of surface potential increases and the decay rate of AC fluctuation voltages is larger than that pure AC. And also, the number of shallow trap with AC fluctuation voltages is larger than that with pure AC. The rate of free charge increases with the number of shallow trap increasing. More free electrons involves in the process of PD, accelerating the aging rate of three-layer oil paper samples. Therefore, it can be concluded that surface charge and trap distribution are helpful to clarify PD mechanism.

INDEX TERMS
On-board traction transformers, PD, surface potential, trap distribution, three-layer oil-paper insulation.

I. NOMENCLATURE

EMUs	Electric multiple units
PD	Partial discharge
ISPD	Isothermal potential decay method
Q_{max}	The max PD charge
N	PD repetition rate
PDIV	Partial discharge inception voltage
t	The decay time
V_s	The surface potential
ε_r	The relative permittivity
ε_0	The permittivity of vacuum
e	The elementary charge
E_t	The trap energy
ν	The attempt to escape frequency
D	The decay rate
V_{3000}	The surface potential at 3000 seconds
V_0	The highest surface potential at t_0
v	The drift velocity
S	The capture cross section of the trap
N_t	The trap density occupied
ν_1	The attempt to escape frequency
dq_{free}/dt	The rate of free charge density
q_{free}	The density of free charge
L	The thickness of the samples
T	The Kelvin temperature
k	The Boltzmann constant
N_t	The trap density occupied by carriers at trap level E
U_0, f_0	The amplitude and frequency of AC

The associate editor coordinating the review of this manuscript and approving it for publication was Pavlos I. Lazaridis.

n_s	The number of shallow trap
dq_{trap}/dt	The rate of trapped charges
q_{trap}	The density of trapped charge
q_e	The center charge
LFO	The low-frequency oscillation
U_j, f_j, φ_j	The amplitude, frequency and phase of LFO
n_d	The number of deep trap

II. INTRODUCTION

On-board traction transformer is an important equipment of energy change in electric locomotives and electric multiple units (EMUs) [1]. Oil-paper insulation plays an important role in insulation of on-board traction transformer [1], which consist of mineral oil and Nomex papers. Among them, Nomex papers with good insulation and heat resistance [2], is used as the interturn insulation of traction winding and the higher voltage winding in on-board traction transformer and is presented the multi-dielectrics structure of interturn insulation. During the actual operation, these interturn insulation due to the electric stress, thermal stress and mechanical stress are prone to appear insulation defects [3], including fracture, metal tip, cavity and so on. They will cause the unevenness of electric field and the concentration of the local electric field. The local irregular electric field may result in charge accumulation on the surface of oil-paper insulation. Finally, Partial discharge (PD) is easy to take place within the above insulation defects and even irremediable damage will appear in the multilayer oil-paper insulation. As a result, the chemical bond groups of Nomex paper is broken and the chemical traps is formed. The traps will further affect the characteristics of charge transport, accumulation and dissipation [6]. Therefore, it is of great significance to investigate the evolution law of trap parameters and its influence mechanism on partial discharge.

Considerable research has been done on PD characteristics and charge transporting characteristics of oil-paper insulation under AC, DC and combined voltage. The PD characteristics and propagation models of different streamers [7] are studied and proposed under AC. The time lag/recovery model is presented and 3-dimensional histogram is suggested to be used as a base for discharge recognition under DC in [8]. In addition, Bao *et al.* [9] have paid much attention to the characteristic and mechanism of PD with combined voltage. They founded that the great difference of PD behavior and mechanisms exists among combined voltage, AC and DC voltage.

Recent research work indicated that surface charge and trap distribution had a great effect on the electrical and mechanical properties of dielectric, and reported that surface charge and trap distribution were the main factor leading to PD degradation. Pan *et al.* [12] discussed the influence of surface charge decay on discharge frequency at DC voltage and concluded that the research is helpful to clarify PD mechanism under DC voltage. Gao *et al.* [13] reported that polypropylene/propylene-based elastomer (PP/PBE) blend has deeper trap depth compared with polypropylene/ polyolefin elastomer (PP/POE) blend, which should be responsible for its higher DC breakdown strength. Sarathi and Sahitya Yadav [14] found that the tensile and flexural strength reduces drastically for thermally aged copper sulphide diffused OIP material compare to unused specimen. Du *et al.* [15] studied the influence different compound voltage on surface charge of epoxy resin, and utilized trap distribution to analyze charge decay process. He also found [17] that the first peak for the $t\mathrm{d}V/dt$ curves is related to a faster decay process of charge escaped from the shallow trap, while the second peak is related to a slower decay process of charge escaped from the deep trap. Liang *et al.* [18] reported that the addition of SiC with non-linear conductivity can effectively alter surface charge distribution, and inferred that the level of deep traps is 0.9 eV and the level of shallow trap is 0.8 eV.

These studies mainly focused on PD characteristics of oil-paper insulation and the properties of surface charge and the qualitative analysis of trap distribution, including trap density and $t\mathrm{d}V/dt$. However, the literature on the evolution of trap parameters and the quantitative analysis of trap distribution during the PD degradation for oil-paper insulation is rare. Besides, we founded that the discharge characteristics of the oil-paper interface and the insulating dielectrics vary with the energy level and density of surface trap at different PD degradation stages, which are based on experimental investigations. Therefore, it is very important to study the evolution of trapping parameters on three-layer oil-paper insulation of PD degradation for on-board traction transformers.

In order to study these effects, the experimental setup of PD and surface charge are carried out. By using isothermal potential decay (ISPD) method, the surface potential at different PD process for three layers oil-paper insulation are measured. On this basis, its trap distribution is calculated. Furthermore, the evolution of trap for oil-paper insulation and the influence of trap distribution on PD are analyzed.

III. EXPERIMENTAL SETUP

A. THE VOLTAGE ANALYSIS IN ON-BOARD TRACTION TRANSFORMER

The characteristics of fluctuated AC voltage and its produced process had minutely described and reported in [1]. As we have described in [1], the higher winding is subjected to a large AC fluctuation voltage stresses consisting of AC, inter-harmonic components, high harmonics components and the transient voltage impulse. Among them, inter-harmonic components are the main reason for unstable supply voltages of the higher winding. These inter-harmonics components can be regarded as the result of amplitude modulation of the low-frequency oscillation (LFO) with a frequency of 3 Hz to 7 Hz on the basis of AC with 50 Hz. As a result, the voltages at these resonant frequencies is amplified and fluctuated frequently between 19 and 31 kV. The waveforms of fluctuation voltages can be seen as shown in Figure 1 and can be

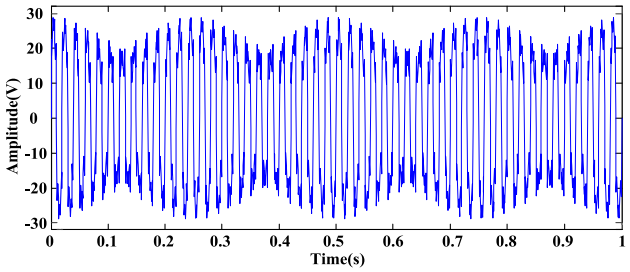

FIGURE 1. Waveforms of HV winding.

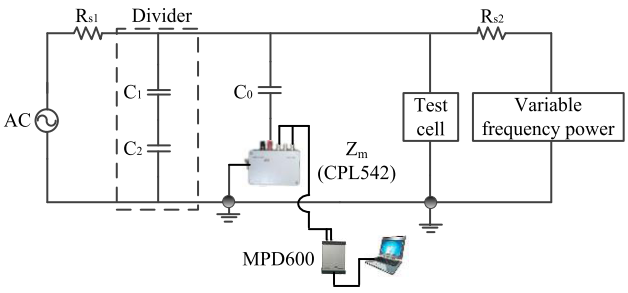

FIGURE 2. Experimental setup.

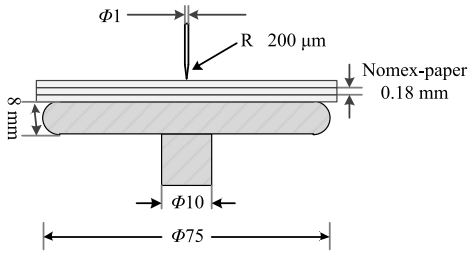

FIGURE 3. Test electrode system.

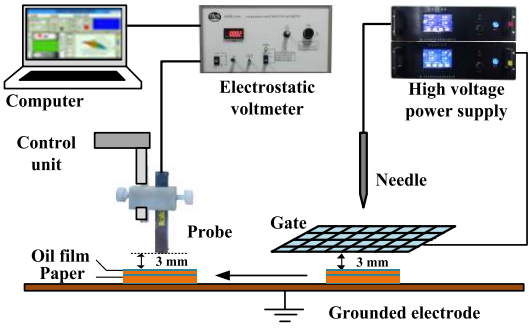

FIGURE 4. Surface potential measuring system.

expressed by Equation (1) in [1]

$$u(t) = U_0 \sin(2\pi f_0 t) + \sum_{j=1}^{N} U_j \sin(2\pi (f_0 + f_j)t + \varphi_j) \quad (1)$$

where U_0 and f_0 denote the amplitude and frequency of AC. U_j, f_j and φ_j represent the amplitude, frequency and phase of LFO.

B. PD MEASUREMENT

The experimental arrangement of PD with AC fluctuation voltages is presented in Figure 2. According to the IEC 60060-3 standard [22], a variable frequency power (54 Hz) is used for generating the inter-harmonic voltage, which forms AC voltage fluctuation impulse. A 10 kVA and 100 kV (50 Hz) corona free test transformer is considered as power source for AC voltage. R_{s1}, R_{s2} denote the current-limiting resistors, with a value of 10 kΩ in [1]. C_1, C_2 are the voltage divider, with the ratio of 1000:1. C_0 is coupling capacitor, with a capacity of 300 pF. In this test, MPD 600 is used for measuring PD signals by a pulse current detection. And also, during the actual operation of on-board traction transformer, insulation defects are prone to appear in interturn of on-board traction transformer due to multi- stresses. In order to imitate the operation condition, a needle-plane model was designed as shown in Figure 3. In the model, Nomex T410 paper produced by DuPont with diameter 80 mm is used. Karamay 25# produced by Kunlun Energy is selected.

C. SURFACE CHARGE MEASUREMENT

Based on PD results, we selected oil-impregnated Nomex papers at different PD stages (i.e. PD degradation samples) to carry out the surface potential test. The surface potential test is shown in Figure 4. The needle electrode is set to 5 mm above the samples [15]. Samples were charged by using corona charging method. In order to obtain uniformly distributed charge, the gate electrode is added between the ground electrode and the needle electrode. The needle electrode and the gate electrode are connected with DC voltage. Its voltage amplitudes are ±8 kV and ±3 kV, respectively. The voltage is applied to the needle electrode and the gate electrode and hold for 10 minute. Then, the samples are rapidly shifted to the probe and insure that the probe is in the same position as needle. An electrostatic voltmeter (trek model 341-b) connected to a Kelvin probe (model: trek-3455-et) was used for measuring the surface potential [15]. The probe is positioned 3 mm above the samples [23]. In this experiment, three layers of paper are stacked together and two layers of oil film can be found among three sheets of paper because the Nomex paper had been impregnated in oil.

D. CALCULATION OF TRAP DISTRIBUTION

Based on the above result, the evolution of trap parameters of PD degradation samples at different stages is obtained. The trap density and energy can be expressed [13]:

$$N_t(E) = \frac{4\varepsilon_0\varepsilon_r}{ekTL^2}\left|t\frac{dV_s(t)}{dt}\right| \quad (2)$$

$$E_t = kT\ln(\nu_1 t) \quad (3)$$

where t is the decay time, V_s is the surface potential, ε_r is the relative permittivity, ε_0 is the permittivity of vacuum, e

is the elementary charge, L is the thickness of the samples, T is the Kelvin temperature, k is the Boltzmann constant, N_t is the trap density occupied by carriers at trap level E, E_t is the trap energy, ν_1 is the attempt to escape frequency and was selected as 10^{12} s^{-1} in this work in [13].

IV. RESULTS

A. PD CHARACTERISTIC

The applied voltage is increased at a rate of 0.5 kV and lasts for 5 minute at each step. The max PD charge (Q_{max}) and PD repetition rate (N) can be obtained in Figure 5 under AC fluctuation voltages and pure AC, respectively.

It can be observed that the similar properties of PD with AC fluctuation voltages and pure AC are shown from PDIV (PD inception voltage) to PD breakdown. The max PD charge increases exponentially with applied voltage increasing. Under AC fluctuation voltages, the max PD charge increases slowly before 14 kV but increase prominently after 14 kV. Under pure AC, it begins to increase prominently after 15 kV. In addition, PD repetition rate varies by hyperbolic tangent under AC fluctuation voltages and pure AC.

However, another interesting observation is that the divergences of PD properties can be found. The max PD charge has no obvious change before 14 kV. After 14 kV, it shows a larger value under AC fluctuation voltages than that under pure AC. Nevertheless, PD repetition rate shows a larger value under pure AC than that AC fluctuation voltages from 9 kV to 12 kV. In particular, PD repetition rate with pure AC enhances prominently before 10 kV. After 11 kV, PD repetition rate increases remarkably under AC fluctuation voltages. Besides, PD duration with AC fluctuation voltages is shorten. These PD results might contribute to the higher dv/dt to vary with the phase caused by the addition of the inter-harmonic to AC as described in the previous work [1].

B. SURFACE POTENTIAL DISTRIBUTION

From the above PD experimental results, it can be seen that the above curves show a clear inflection point, that is 10 kV, 12 kV and 14 kV. We selected the PD degradation samples at 10 kV, 12 kV and 14 kV to perform surface potential test. It should be noted that the needle in the surface potential measuring system is aligned to the position of the needle in PD experiment. The samples were charged by using the negative corona discharge mode. After the charging, the samples were quickly moved to probe for measurement [23]. The measurement results are shown in Figure 6.

It can be seen in Figure 6 that the decay of surface potential is fast at the initial period, and then gradually becomes slower with the time [17]. The decay of surface potential on three-layer oil-paper sample of PD degradation at 14 kV is greater than that at 12 kV, 10 kV and untreated sample. It can be found that the decay of untreated sample is the slowest. After PD degradation, the insulating property of three-layer oil-paper insulation gradually deteriorates, resulting in the decay degree of corresponding sample increases. In other words, the surface potential decay of the three-layer oil-paper sample increases with the increase of PD degradation. It is also observed that the difference in initial surface potential of samples under pure AC and AC fluctuation voltages is obvious in curves. And also, the decay degree on samples of PD degradation under AC fluctuation voltages is greater than that under pure AC.

In order to study the effect of the decay rate on PD of three layer oil-paper insulation, the decay rate of surface potential

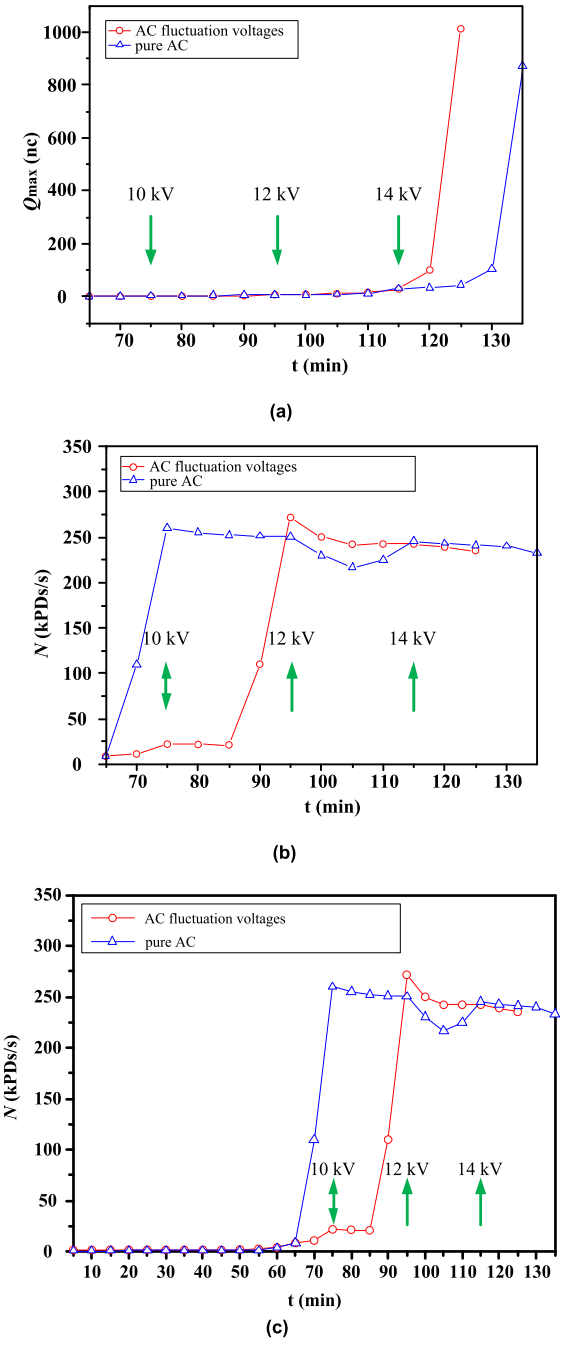

FIGURE 5. PD characteristics under AC fluctuation voltages and pure AC. (a) Qmax. (b) N from PDIV to PD breakdown. (c) N from zero to PD breakdown.

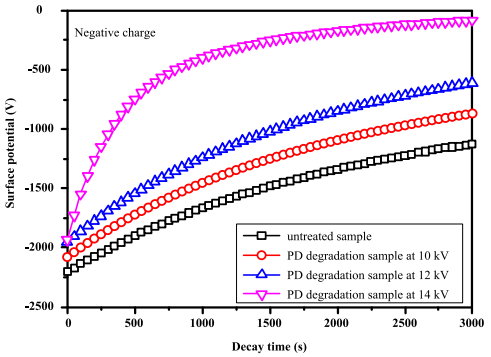

(a)

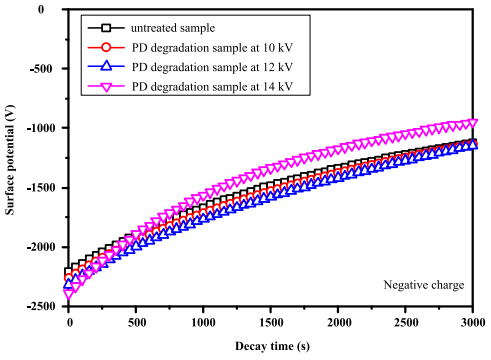

(b)

FIGURE 6. The curves of surface potential, after PD degradation. (a) under AC fluctuation voltages. (b) under pure AC.

is defined as follows [25]:

$$D = \frac{V_{3000} - V_0}{V_0} \tag{4}$$

where D is the decay rate, V_{3000} is the surface potential at 3000 seconds, V_0 is the highest surface potential at t_0 [23]. According to the above formula, the curves of decay rate for surface potential of three-layer oil-paper at different PD stages is plotted in Figure 7. It is clearly shown that the decay rate surface potential with AC fluctuation voltages increases from 49 % to 96 %. While the decay rate surface potential with pure AC increases from 49 % to 60 %. That is to say, the decay rate of surface potential with AC fluctuation voltages is higher than that with pure AC. The reasons for these are that AC fluctuation voltages generates the higher dv/dt caused by inter-harmonic components [1, 24]. These higher dv/dt release more energy in PD degradation, indicating that the trapped charges in traps are easy to escape and accelerate the decay of surface potential and the migration velocity of electrons.

C. TRAP DISTRIBUTION

Based on the results of surface potential, the trap energy distributions of carrier for samples with PD degradation can be obtained as shown in Figure 8(a) and Figure 8(b), which were calculated from the equations of (2) and (3).

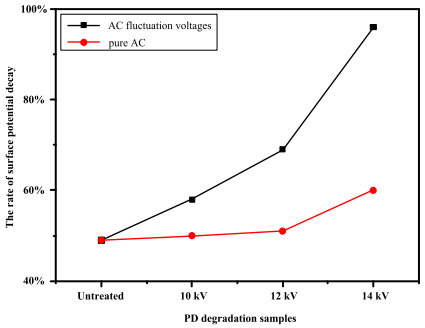

FIGURE 7. The decay rate of surface potential at different PD degradation.

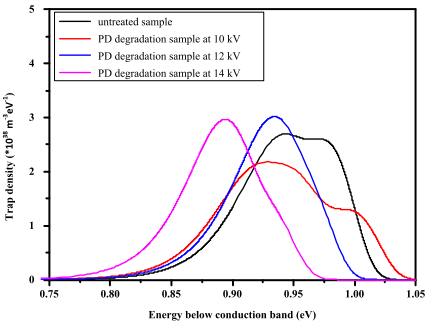

(a)

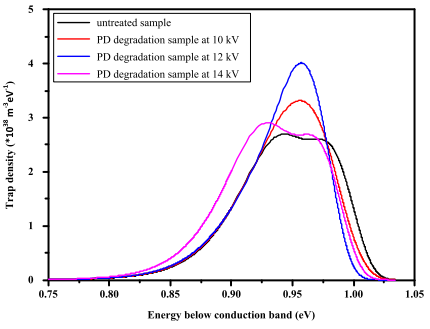

(b)

FIGURE 8. Trap distributions of oil-paper samples after PD experiment. (a) AC fluctuation voltages. (b) under pure AC.

As can be seen from Figure 8, for untreated sample, the curves of trap distribution has two peaks: shallow trap and deep trap, in which the trap distribution is dominated by deep trap. After PD occurs, the peak of curves on PD degradation samples becomes a peak basically. The value of trap depth for PD degradation samples is smaller compared with untreated sample. The curves of trap distribution shifts to the left with the applied voltage increasing. It means that the value of trap depth decreases and the number of shallow trap increases, which reflects a faster decay process. When the applied voltage reaches 14 kV, the lower value of trap depth for PD degradation samples is, the more number of shallow traps is, the higher remarkable decay rate of surface potential is. It illustrates that the change of trap at PD different stages is related to the characteristic of charge transport.

After PD occurs, the electric field is strengthened with the increase of applied voltage. The charges get more energy to transfer, trap & detrap and recombine. In this case, a large number of energy is released, resulting in bond-breaking, cross-linking, coupling, curling of macromolecular chains in the three-layer oil-paper samples. And also, new groups is generated and a large number of shallow traps is formed. Besides, when the value of trap depth decreases, many charges trap in shallow traps and charges detrap more easily. As a result, the decay rate of surface potential increases. More free electrons involves in the process of PD, accelerating the aging rate of three-layer oil paper samples.

However, it is also observed that the considerable divergence of trap distribution for PD degradation samples between pure AC and AC fluctuation voltages can be found. The values of trap density and level for shallow trap and deep trap are different. i.e. These specimens, the density of trap and the value of trap depth under AC fluctuation voltages is lower than that under pure AC. The ranges of shallow trap level of samples are about 0.75-0.95 eV. While the ranges of deep trap level of samples are about 0.95-1.05 eV. In order to quantify and analyze the rules of the number of shallow and deep trap (i.e. the trap density), we employ the integral method to calculate the number of shallow and deep trap in the range of 0.75-0.95 eV and 0.95-1.05 eV, respectively. The number of shallow and deep trap can be expressed respectively:

$$n_s = \int_{0.75}^{0.95} N_t(E)dE \tag{5}$$

$$n_d = \int_{0.95}^{1.05} N_t(E)dE \tag{6}$$

where, n_s is the number of shallow trap, and n_d is the number of deep trap. The number of shallow and deep trap we obtained are given in figure 9.

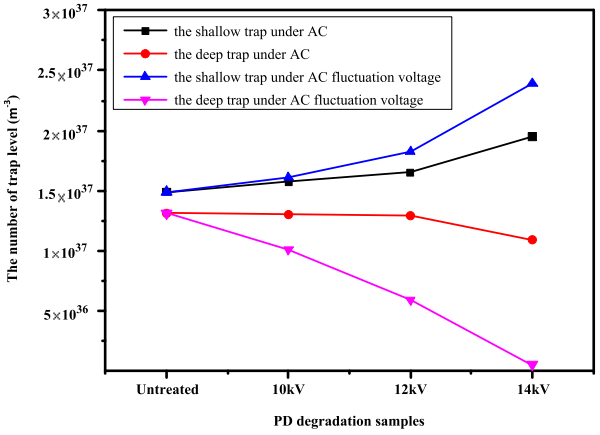

FIGURE 9. The number of trap with three-layer oil-paper samples after PD.

It is clearly shown that the number of deep traps decreases and the number of shallow traps increases. The number of shallow traps under pure AC is lower than that under AC fluctuation voltage. And also, the number of shallow traps under pure AC increases from $1.49*10^{37}$ m^{-3} to $1.5*10^{37}$ m^{-3}. The number of deep traps under AC fluctuation voltage increases from $1.49*10^{37}m^{-3}$ to $2.39*10^{37}$ m^{-3}. Another interesting feature that the number of deep traps under pure AC is much more than two orders of magnitude that under AC fluctuation voltage. The number of deep traps under pure AC drops from $1.31*10^{37}m^{-3}$ to $1.09*10^{37}$ m^{-3}. While the number of deep traps under AC fluctuation voltage drops from $1.31*10^{37}$ m^{-3} to $5*10^{35}$ m^{-3}. These are because the higher dv/dt caused by AC fluctuation voltage produces more energy to accelerate the process of electron detrapping. As a result, more free electrons involves in the process of PD, accelerating the aging rate of three-layer oil paper samples.

V. DISCUSSION

A. ELECTRIC FIELD EVOLUTION DURING PD PROCESS

Generally, the electric field and seed electrons supply are responsible for the change of PD characteristics. The surface charge decay and trap distribution may be responsible for the field and seed electrons supply. It can be seen in Figure 5a), Figure 7 and Figure 9 that the same property, i.e. the field dependent property, can be obtained. Based on the above results, we divide the electric field into the following ranges: the low electric field (1 kV to 10 kV), the moderate electric field (10 kV to 14 kV), and the high field (14 kV to 16 kV). A field-dependent model of dominant charge transport behavior is putted forward as shown in Figure 10.

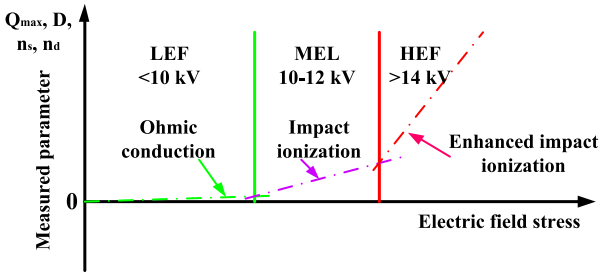

FIGURE 10. Field dependence model of dominant charge behavior.

Under a low electric field, the max PD charge, the decay rate of surface potential, and the number of shallow and deep trap show a slightly increasing trend with the increase of applied voltage, which corresponds to an Ohmic conduction. This is mainly due to the fact that a critical field PD take place has not been reached. And also, the charge injected from needle electrode accumulated on the surface of oil-impregnated Nomex paper. It will suppress the occurrence of PD. That is to say, there is basically not a single one or several carrier migration mechanisms that are in domination.

An electric field in the range from 10 kV to 14 kV is considered to be a moderate electric field for our experimental setup. In this case, a critical field PD take place is exceeded. The charged particles in the ionization were pushed by the field which have the horizontal and perpendicular component to the surface and gradually trapped on the surface. The

charges injected at the surface of oil-paper insulation increase linearly. These charges increased migrate along the surface of Nomex paper and provide seed electrons for the development of PD. As a results, the decay rate of surface potential and the number of shallow trap increase linearly.

When the electric field exceeds 14 kV, the charging property of oil-paper is dominated by the enhanced impact ionization. A large amount of charge is injected at the bulk and surface of oil-paper. The charge quickly migrate along the bulk and surface of Nomex paper and accelerate the development of PD. As a results, the decay rate of surface potential and the number of shallow trap increase exponentially.

B. THE EFFECT OF HIGHER DV/DT

The above results indicated that PD distribution, surface charge distribution and trap distribution are related to the higher dv/dt. As described in [1], the addition of the inter-harmonic to AC leads to variation of peak voltage and time derivative dv/dt along the phase. It is noteworthy that these facts are influential in PD distribution, surface charge distribution and trap distribution.

In order to analyze the effect of higher dv/dt caused by fluctuated AC voltage, the local graph under pure AC and AC fluctuation voltages are plotted in Figure 11. It is clearly shown that higher crest is appeared in AC fluctuation voltages compared with pure AC and its crest value varies with time. Thus, the higher crest makes the change of the surface charge and the electric field as shown in Figure 12. It will further affect the PD characteristics. That is to say, the higher dv/dt intensifies the ionization degree of particles, resulting in the enhancement of trapped charge. The charge enhanced will accelerate the decay of and migration of surface charge along the surface and bulk of Nomex paper. This indicates that the discharge time interval between two adjacent PDs and the development of PD are shorten. PD makes gradually the aging and degradation of oil-paper insulation. From microcosmic aspect, the chemical bond of oil-paper insulation is broken and the trap distribution is altered.

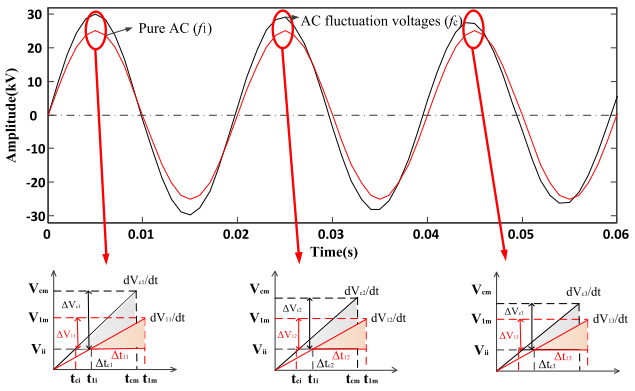

FIGURE 11. Local graph of AC fluctuation voltages and AC voltage.

As a results, the number of shallow traps under AC fluctuation voltage is higher than that under pure AC. The number

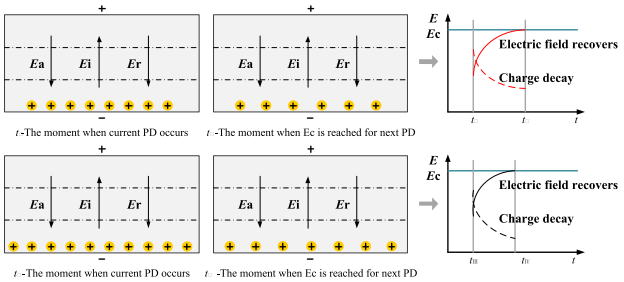

FIGURE 12. The effect of higher dv/dt on PD and surface charge decay. (a) under pure AC. (b) AC fluctuation voltages.

of deep traps under AC fluctuation voltage is much lower than that under pure AC (Figure 8 and Figure 9). It indicates that more free electrons involves in the process of PD, accelerating the aging rate of three-layer oil paper samples. The discharges comes to these higher crest value and the duration of PD under AC fluctuation voltages is lower than those pure AC (Figure 5), which is consistent with [1].

C. THE EFFECT OF TRAP DISTRIBUTION ON PD

The charge carried away by an external electric field, then will be captured by the trap and stay in the trap. The probability of charge trapping is Pin [25], and the probability of charge detrapping is Pout [26]

$$P_{\text{in}} = \nu S N_{\text{t}} \tag{7}$$

$$P_{\text{out}} = \nu_1 \exp(-E_{\text{t}}/kT) \tag{8}$$

where, ν is the drift velocity, S is the capture cross section of the trap, N_{t} is the trap density occupied, ν_1 is the attempt to escape frequency, and E_{t} is the trap energy.

The process of trapping or detrapping in trap during charge transportation can be described by a first-order kinetic charge trapping/detrapping model [27]

$$\frac{\mathrm{d}q_{\text{free}}}{\mathrm{d}t} = -P_{\text{in}} q_{\text{free}} \left(1 - \frac{q_{\text{trap}}}{q_{\text{e}} N_{\text{t}}}\right) + P_{\text{out}} q_{\text{trap}} \tag{9}$$

$$\frac{\mathrm{d}q_{\text{trap}}}{\mathrm{d}t} = P_{\text{in}} q_{\text{free}} \left(1 - \frac{q_{\text{trap}}}{q_{\text{e}} N_{\text{t}}}\right) - P_{\text{out}} q_{\text{trap}} \tag{10}$$

where, $\frac{\mathrm{d}q_{\text{free}}}{\mathrm{d}t}$ is the rate of free charge density, q_{free} is the density of free charge, $\frac{\mathrm{d}q_{\text{trap}}}{\mathrm{d}t}$ is the rate of trapped charges, q_{trap} is the density of trapped charge, and q_{e} is the center charge.

Substituting equations (7) and (8) into equations (9) and (10), we can get:

$$\frac{\mathrm{d}q_{\text{free}}}{\mathrm{d}t} = -\nu S q_{\text{free}} \left(N_{\text{t}} - \frac{q_{\text{trap}}}{q_{\text{e}}}\right) + \nu_1 \exp\left(-\frac{E_{\text{t}}}{kT}\right) q_{\text{trap}} \tag{11}$$

$$\frac{\mathrm{d}q_{\text{trap}}}{\mathrm{d}t} = \nu S q_{\text{free}} \left(N_{\text{t}} - \frac{q_{\text{trap}}}{q_{\text{e}}}\right) - \nu_1 \exp\left(-\frac{E_{\text{t}}}{kT}\right) q_{\text{trap}} \tag{12}$$

From equation (11) and (12), it can be seen that the process of charge trapped and detrapped is related to trap energy and trap density. When trap energy decreases, the probability of charge detrapping increases and the rate of free

charge increases. It indicates that the rate of charge trapped decreases and the number of free charges increases, which helps the migration of charges in oil paper. When trap density decreases, the probability of charge trapping decreases and the rate of free charge increases. It indicates that the rate of charge trapped decreases and the number of free charges increases, which helps the migration of charge.

Through analysis, it can be found that the trap energy of three-layer oil-paper samples after PD degradation decreases with the applied voltage increasing, resulting in the enhancement of free charge rate. More charges are not bound by the trap and participate in the development of PD, indicating that the severity of the discharge increases and the decay rate of charge increases (Figure 7). It will make the samples is destroyed to form a large number of shallow traps (Figure 9). The carrier is trapped in these shallow traps to overcome the lower energy barrier and is more likely to migrate between the two traps [24]. Furthermore, the superposition of the inter-harmonic to AC leads to variation of peak voltage and generates the higher dv/dt. These higher dv/dt will lead to the differences between AC fluctuation voltages and AC. Namely, the higher the severity of the discharge with AC fluctuation voltages is, the faster the rate of charge decay is, the worse the extent of damage is, and the more the number of shallow traps than that pure AC is.

Moreover, with the applied voltage increasing, the electric field is enhanced and the effect of dv/dt on PD is strengthened. This strengthened field and higher dv/dt makes more charges migrating across the surface and bulk of three-layer oil paper and these higher dv/dt release more energy in PD degradation. More charges are involved in partial discharge and the charges get more energy in the process of transferring, trapping & detrapping and recombining, resulting in macromolecular chains fracture on PD degradation samples. The value of trap depth decreases and a large number of shallow traps is formed. Many charges is trapped in shallow traps and these charges trapped in shallow traps is easy to detrap and accelerate the decay of surface potential. It indicates that surface potential decay on PD degradation sample increases with the applied voltage increasing. And also, the decay rate of degradation samples with AC fluctuation voltages is larger than that with pure AC (Figure 6 and Figure 7). Besides, the value of trap depth decreases and the number of shallow trap increases with the increase of PD degradation. The value and number of trap depth with AC fluctuation voltages is lower than that with pure AC (Figure 8 and Figure 9).

VI. CONCLUSION

The conclusions are obtained as follows:

(1) The decay of surface potential for the three-layer oil-paper samples increases with the increase of PD degradation under AC fluctuation voltages and AC fluctuation voltages. It is also observed that the decay rate of surface potential with AC fluctuation voltages is higher than that with pure AC. The reason is that the higher dv/dt caused by AC fluctuation voltages releases more energy to accelerate the decay of surface potential and the migration velocity of electrons.

(2) The curve of trap distribution shifts to the left with the gradual degradation of samples. It indicates that the number of shallow trap increases and the number of deep trap decreases with the gradual degradation of samples, which reflects a faster decay process. However, it is also observed that the number of shallow trap under AC fluctuation voltages is larger than that under pure AC but the number of deep trap is lower.

(3) The higher dv/dt accelerates the decay rate of surface charge and the migration velocity of electrons, resulting in the enhancement of free charge rate. More free charges participate in the development of PD to accelerate the degradation of samples.

(4) We can conclude that the characteristic of charge transportation is an important reason for the evolution of trap distribution in PD degradation of three-layer oil paper.

REFERENCES

[1] X. Li, G. Wu, Y. Yang, Z. Wang, P. Xu, Y. Li, and B. Gao, "Partial discharge characteristics of oil-paper insulation for on-board traction transformers under superposed inter-harmonic AC voltages," *IEEE Trans. Dielectr. Electr. Insul.*, vol. 27, no. 1, pp. 240–248, Feb. 2020.

[2] M. Wen, J. Song, Y. Song, Y. Liu, C. Li, and P. Wang, "Reliability assessment of insulation system for dry type transformers," *IEEE Trans. Dielectr. Electr. Insul.*, vol. 20, no. 6, pp. 1998–2008, Dec. 2013.

[3] S. Li, G. Gao, G. Hu, B. Gao, H. Yin, W. Wei, and G. Wu, "Influences of traction load shock on artificial partial discharge faults within traction transformer—Experimental test for pattern recognition," *Energies*, vol. 10, no. 10, pp. 1–17, Oct. 2017.

[4] L. Zhou, D. Wang, L. Guo, L. Wang, J. Jiang, and W. Liao, "FDS analysis for multilayer insulation paper with different aging status in traction transformer of high-speed railway," *IEEE Trans. Dielectr. Electr. Insul.*, vol. 24, no. 5, pp. 3236–3244, Oct. 2017.

[5] R. Sarathi and G. Koperundevi, "Investigation of partial discharge activity of single conducting particle in transformer oil under DC voltages using UHF technique," *IET Sci., Meas. Technol.*, vol. 3, no. 5, pp. 325–333, Sep. 2009.

[6] H.-B. Mu, G.-J. Zhang, Y. Komiyama, S. Suzuki, H. Miyake, Y. Tanaka, and T. Takada, "Investigation of surface discharges on different polymeric materials under HVAC in atmospheric air," *IEEE Trans. Dielectr. Electr. Insul.*, vol. 18, no. 2, pp. 485–494, Apr. 2011.

[7] D. Swaffield, P. Lewin, G. Chen, and S. Swingler, "Partial discharge characterization of streamers in liquid nitrogen under applied AC voltages," *IEEE Trans. Dielectr. Electr. Insul.*, vol. 15, no. 3, pp. 635–646, Jun. 2008.

[8] U. Fromm, "Interpretation of partial discharges at DC voltages," *IEEE Trans. Dielectr. Electr. Insul.*, vol. 2, no. 5, pp. 761–770, Nov. 1995.

[9] L. Bao, J. Li, J. Zhang, T. Jiang, and X. Li, "Partial discharge process and characteristics of oil-paper insulation under pulsating DC voltage," *J. Electr. Eng. Technol.*, vol. 11, no. 2, pp. 436–444, Mar. 2016.

[10] L. Bao, J. Li, J. Zhang, X. Li, and X. Li, "Influences of temperature on partial discharge behavior in oil-paper bounded gas cavity under pulsating DC voltage," *IEEE Trans. Dielectr. Electr. Insul.*, vol. 23, no. 3, pp. 1482–1490, Jun. 2016.

[11] J. Li, Z. He, and S. Grzybowski, "Electrical aging lifetime model of oil-impregnated paper under pulsating DC voltage influenced by temperature," *IEEE Trans. Dielectr. Electr. Insul.*, vol. 20, no. 6, pp. 1992–1997, Dec. 2013.

[12] C. Pan, W. Song, J. Tang, Y. Luo, and J. Yin, "Influence of surface charge decay on cavity PD frequency at DC voltage," *IET Sci., Meas. Technol.*, vol. 13, no. 2, pp. 193–200, Mar. 2019.

[13] Y. Gao, J. Li, Y. Yuan, S. Huang, and B. Du, "Trap distribution and dielectric breakdown of isotactic polypropylene/propylene based elastomer with improved flexibility for DC cable insulation," *IEEE Access*, vol. 6, pp. 58645–58661, 2018.

[14] R. Sarathi, K. S. Yadav, and M. Swarna, "Understanding the surface discharge characteristics of thermally aged copper sulphide diffused oil impregnated pressboard material," *IEEE Trans. Dielectr. Electr. Insul.*, vol. 22, no. 5, pp. 2513–2521, Oct. 2015.
[15] B. X. Du, A. Li, and J. Li, "Effects of AC and pulse voltage combination on surface charge accumulation and decay of epoxy resin," *IEEE Trans. Dielectr. Electr. Insul.*, vol. 23, no. 4, pp. 2368–2376, Aug. 2016.
[16] B. X. Du and A. Li, "Effects of DC and pulse voltage combination on surface charge dynamic behaviors of epoxy resin," *IEEE Trans. Dielectr. Electr. Insul.*, vol. 24, no. 4, pp. 2025–2033, Jan. 2017.
[17] B. X. Du, J. P. Jiang, J. G. Zhang, and D. S. Liu, "Dynamic behavior of surface charge on double-layer oil-paper insulation under pulse voltage," *IEEE Trans. Dielectr. Electr. Insul.*, vol. 23, no. 5, pp. 2712–2719, Oct. 2016.
[18] H. Liang, B. Du, J. Li, Z. Li, and A. Li, "Effects of nonlinear conductivity on charge trapping and de-trapping behaviors in Epoxy/SiC composites under DC stress," *IET Sci., Meas. Technol.*, pp. 83–89, Sep. 2017.
[19] J. Holtz and H.-J. Kelin, "The propagation of harmonic currents generated by inverter-fed locomotives in the distributed overhead supply system," *IEEE Trans. Power Electron.*, vol. 4, no. 2, pp. 168–174, Apr. 1989.
[20] H. Cui, H. Fang, W. Song, X. Feng, and X. Ge, "Resonant harmonic elimination PWM based high-risk harmonic resonance suppression in autotransformer fed electrified railway," in *Proc. 7th IET Int. Conf. Power Electron., Mach. Drives (PEMD)*, 2014, pp. 1–5.
[21] H. Wang, W. Mingli, and J. Sun, "Analysis of low-frequency oscillation in electric railways based on small-signal modeling of vehicle-grid system in dq frame," *IEEE Trans. Power Electron.*, vol. 30, no. 9, pp. 5318–5330, Sep. 2015.
[22] *High Voltage Test Techniques Part 3: Definitions and Requirements for On-Site Tests*, IEC Standard 60060-3, 2005.
[23] S. Kumara, B. Ma, Y. V. Serdyuk, and S. M. Gubanski, "Surface charge decay on HTV silicone rubber: Effect of material treatment by corona discharges," *IEEE Trans. Dielectr. Electr. Insul.*, vol. 19, no. 6, pp. 2189–2195, Dec. 2012.
[24] R. Toomer and T. J. Lewis, "Charge trapping in corona-charge polyethylene films," *J. Phys. D, Appl. Phys.*, vol. 13, no. 7, pp. 1343–1356, Nov. 2000.
[25] A. J. Vandermaar, M. Wang, J. B. Neilson, and K. D. Srivastava, "The electrical breakdown characteristics of oil-paper insulation under steep front impulse voltages," *IEEE Trans. Power Del.*, vol. 9, no. 4, pp. 1926–1935, Nov. 1994.
[26] S. L. Roy, P. Segur, G. Teyssedre, and C. Laurent, "Description of bipolar charge transport in polyethylene using a fluid model with a constant mobility: Model prediction," *J. Phys. D, Appl. Phys.*, vol. 37, no. 2, pp. 298–305, Dec. 2003.
[27] J. M. Alison and R. M. Hill, "A model for bipolar charge transport, trapping and recombination in degassed crosslinked polyethene," *J. Phys. D, Appl. Phys.*, vol. 27, no. 6, pp. 1291–1299, Jan. 1999.
[28] D. R. Wolters and J. J. van der Schoot, "Kinetics of charge trapping in dielectrics," *J. Appl. Phys.*, vol. 58, no. 2, pp. 831–837, Jul. 1985.
[29] C. Li, J. Hu, C. Lin, and J. He, "The control mechanism of surface traps on surface charge behavior in alumina-filled epoxy composites," *J. Phys. D, Appl. Phys.*, vol. 49, no. 44, Nov. 2016, Art. no. 445304.

QUANFU LI was born in Shanxi, China, in 1965. He received the M.Sc. degree in vehicle engineering from Southwest Jiaotong University, Chengdu, China, where he is currently pursuing the Ph.D. degree in vehicle engineering with the State Key Laboratory of Traction Power. He is currently a Senior Engineer in railway vehicle with China Shenhua Railway Equipment Company Ltd., Beijing, China. His research interests include operation management of railway vehicle and condition assessment of equipment.

XIAONAN LI was born in Gansu, China, in 1988. She received the B.Sc. degree in automation and the M.Sc. degree in control engineering from Lanzhou Jiaotong University, Lanzhou, China, in 2011 and 2014, respectively. She is currently pursuing the Ph.D. degree in high voltage and insulation technology with the School of Electrical Engineering, Southwest Jiaotong University, Chengdu, China. From 2014 to 2017, she has worked with the Northwest University for Nationalities, China. Her research interests include condition monitoring, assessment, and fault diagnosis of high-voltage power equipment.

YAN YANG (Member, IEEE) was born in Sichuan, China, in 1984. She received the B.Sc. and Ph.D. degrees in electrical engineering from Xi'an Jiaotong University, Xi'an, China, in 2005 and 2010, respectively. From 2010 to 2015, she has worked with the State Grid Chongqing Electric Power Research Institution, China. She is currently a Lecturer with the School of Electrical Engineering, Southwest Jiaotong University, Chengdu, China. Her research interests include dielectric property and condition assessment of transformer.

YIXUAN LI was born in Henan, China, in 1997. She received the B.Sc. degree in electrical engineering and automation from Huadong Jiaotong University, Nanchang, China, in 2018. She is currently pursuing the M.Sc. degree in electrical engineering with the School of Electrical Engineering, Southwest Jiaotong University, Chengdu, China. Her research interests include dielectric property and condition assessment of transformer.

GUANGNING WU (Fellow, IEEE) was born in Nanjing, China, in 1969. He received the B.Sc., M.Sc., and Ph.D. degrees in electrical engineering from Xi'an Jiaotong University, Xi'an, China, in 1991, 1994, and 1997, respectively. He is currently a Professor of electrical engineering with the School of Electrical Engineering, Southwest Jiaotong University, Chengdu, China. He mainly engages in the research field of high-voltage and insulation technology. His research interests include condition monitoring, fault diagnosis, and insulation life-span evaluation for electrical equipment. He is a Distinguished Professor of the Cheung Kong Scholar. He was a recipient of the National Science Fund for Distinguished Young Scholar.